

Strong optical nonlinearities in gallium and indium selenides related to inter-valence-band transitions induced by light pulses

A. Segura, J. Bouvier,* M. V. Andrés, F. J. Manjón, and V. Muñoz

Institut de Ciència dels Materials, Universidad de Valencia, c/ Dr. Moliner 50, 46100 Burjassot, Valencia, Spain

(Received 8 November 1996; revised manuscript received 1 April 1997)

A nonlinear optical effect is shown to occur in gallium and indium selenides at photon energies of the order of 1.5 eV. It corresponds to transitions from a lower-energy valence band to the uppermost one when a nonequilibrium degenerate hole gas is created in the latter by a laser pulse. This inter-valence-band transition is allowed by crystal symmetry. Its oscillator strength is estimated through the *f*-sum rule and turns out to be about two orders of magnitude higher than that of the fundamental transition. The intensity of this effect is stronger when the pump pulse photon energy is close to that of the inter-valence-band transition; a condition that can be fulfilled only in indium selenide. The transient behavior of the sample transmittance is shown to be controlled by the balance between absorption and stimulated emission, which depends on the hole quasi-Fermi level and the gap renormalization due to Coulomb interaction in the electron-hole gas generated by the pump. [S0163-1829(97)00131-8]

I. INTRODUCTION

Gallium selenide (GaSe) is a III–VI layered semiconductor that has been widely investigated during the last few years due to its outstanding nonlinear optical properties. Results on harmonic generation,^{1–6} parametric oscillation,⁷ or frequency mixing^{8–10} in the near and middle infrared, as well as effects related to excitonic optical nonlinearities giving rise to optical bistability,^{11–15} can be found in the literature. Indium selenide (InSe), belonging to the same family, has also been investigated as a frequency doubler in the middle infrared.¹⁵

Both compounds have very similar linear optical properties. Their absorption spectra are shown in Fig. 1. They exhibit the same structures and intensity, only shifted by the band-gap energy difference (about 0.76 eV at 300 K).^{16–24} About 1.15 and 1.5 eV below the uppermost valence band, with Se *p_z* symmetry, two deeper bands do exist in both materials, with Se *p_x-p_y* symmetry, as shown in the inset of Fig. 1. Valence bands are split by crystal-field anisotropy and spin-orbit interaction.²¹ The transition between those deeper bands and the uppermost one is symmetry allowed for light polarization perpendicular to the *c* axis of the crystal, but cannot be observed in the linear optical regime. In this paper, we show however, that this transition can be observed when the top of the uppermost valence band is emptied by a light pulse, giving rise to strong nonlinear optical effects. In Sec. II, we report the experimental setup. Sec. III is devoted to experimental results, which are discussed and interpreted in Sec. IV.

II. EXPERIMENT

GaSe and InSe monocrystals were grown by the Bridgman method, from a stoichiometric melt in the case of GaSe and from a In_{1.05}Se_{0.95} melt in the case of InSe. The quality of the crystals was tested through the temperature dependence of the exciton absorption peak width. The full width at half maximum (FWHM) of the exciton exhibits a lattice-

controlled dependence in the range from 300 to 77 K and attains at 77 K a value of the order of 5–6 meV for GaSe and 7–8 meV for InSe, which is close to those reported in the literature for high-purity samples.^{17,18}

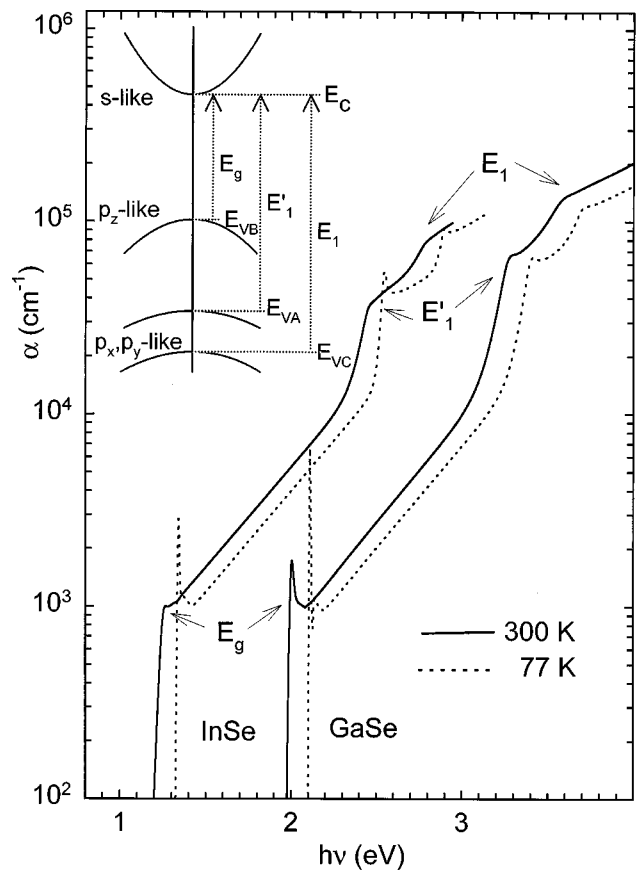


FIG. 1. Absorption coefficient spectra of InSe and GaSe in the spectral range from 1.2 to 4 eV, at 300 and 77 K. Inset: band scheme with the currently accepted assignment of the absorption edges observed in the spectra to electronic transitions (Refs. 21 and 22).

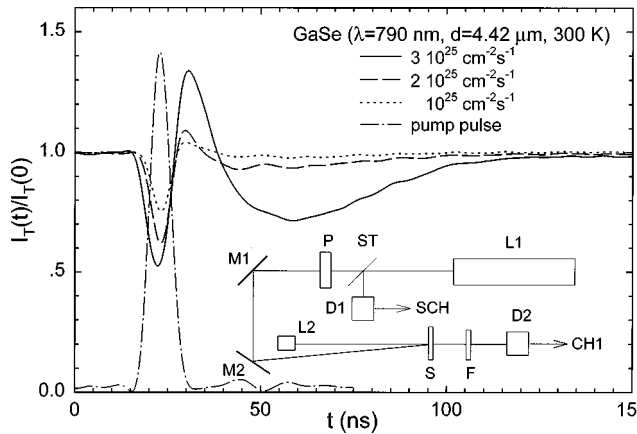


FIG. 2. Transmittancy transients of a 4.42- μm -thick GaSe sample for a 790-nm probe beam, when excited by 532 nm pump pulses with maximum photon fluxes of 1, 2, and 3×10^{25} photons/ cm^2 s. Dotted line: transient intensity of the pump pulse. Inset: experimental setup.

Samples with mirrorlike surfaces parallel to the layers were cleaved from the ingots with a razor blade and cut into slabs 4×4 mm² in size and 2–30 μm thick. The crystal anisotropy axis (*c* axis) is perpendicular to the layers in both semiconductors. Samples were mounted in an aluminum holder with several holes and stuck to it with silver paste in order to improve the thermal contact. The sample holder could be heated up to 100 °C. The optical setup is shown in the inset of Fig. 2. A cw 3-mV GaAs laser diode mounted on a Peltier element (so as the wavelength could be tuned from 780 to 805 nm) generates the probe beam. The probe beam was collimated with a 10 \times microscope objective with 15 mm focal length provided with a diaphragm with a 1 mm diameter placed at 10 mm from the laser diode. The collimated probe beam crosses the sample parallel to the *c* axis and reaches a Si photodetector with a bandwidth of 180 MHz, whose response is monitored by a computer-controlled 400-MHz bandwidth oscilloscope. Signal-to-noise ratio was improved by using the averaging capabilities of the oscilloscope. The pump beam is the second harmonic of a 10 ns Nd-YAG (yttrium aluminum garnet) pulsed laser or a Ti-sapphire laser pumped by the former. In both cases the pump signal is suppressed by an optical filter. When the Ti-sapphire pulse is nearly in resonance with the probe, the pump signal attaining the detector is previously recorded (without the probe) and subtracted from the pump/probe transient. The diameter of the pump laser beam was 3 mm. The energy per pulse impinging on the sample was limited to 3 mJ in most experiments, corresponding to a photon flux of the order of 3×10^{25} cm⁻² s⁻¹ at the pump pulse maximum, for both pump lasers (the lower photon energy in the Ti-sapphire laser is compensated by the longer duration of the pulse).

III. RESULTS

All transient responses shown in this section have been normalized to the probe intensity transmitted by the sample in absence of excitation. Figure 2 shows the time response of the probe intensity transmitted by a 4.42 μm -thick GaSe sample when excited by 532 nm pump pulses with different

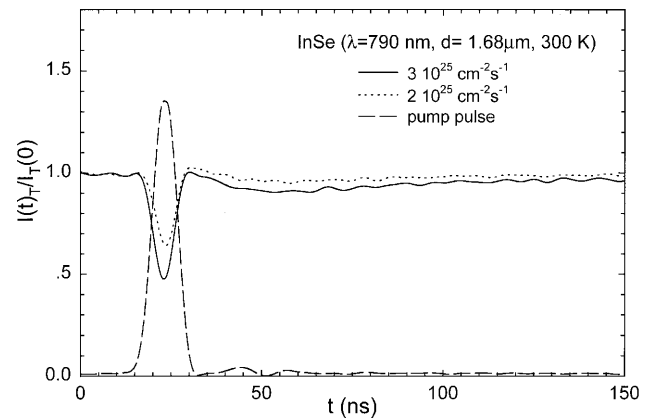


FIG. 3. Transmittancy transients of a 1.68- μm -thick InSe sample for a 790-nm probe beam, when excited by 532-nm pump pulses with maximum photon fluxes of 2 and 3×10^{25} photons/ cm^2 s. Dotted line: transient intensity of the pump pulse.

energies. The probe laser wavelength was 790 nm and the corresponding photon energy, 1.569 eV, is lower than the GaSe band gap, 2.02 eV at room temperature (RT). The probe wavelength being close to an interference maximum, the sample transmittance in absence of excitation, is about 93%. Losses are mainly due to the scattering of the probe beam by surface imperfections. Three stages can be distinguished in the time response of Fig. 2. In the first stage, roughly corresponding to the rise of the pump pulse, the transmitted intensity decreases down to a value of 50% of the initial one (full curve in Fig. 2). At higher pump intensities it can be as low as 20% of the initial value (full curve in Fig 5). If this intensity decrease is due to a transient absorption of the probe beam, then a transmittance of 50 to 20% corresponds to an absorption coefficient of 1500–3500 cm⁻¹. In the second stage, the intensity abruptly increases reaching a value that can be 30–50 % higher than the initial one. This stage corresponds to the fall of the pump pulse, but starts before the pulse reaches its maximum when the pump photon flux is of the order of 3×10^{25} cm⁻² s⁻¹. In the third stage, the transmitted intensity decreases again, reaches a new minimum, and then slowly increases to recover the initial value. This stage starts at the end of the exciting pulse and can last as long as 90 ns. Some structures superimposed to the slow response, appearing in this stage, correspond to secondary pulses of the pump. At low pump pulse energies, only the first stage is observed.

The time response shown in Fig. 3 has been taken in the same conditions as that in Fig. 2, but the sample is a 1.68 μm -thick InSe slab. In this case, the sample must be very thin because the photon energy of the probe beam is above the InSe absorption edge. The linear absorption coefficient is 1500 cm⁻¹ and the sample transmits about 50% of the probe intensity. The structure of the transient is similar to that of Fig. 2, besides the fact that the increase in the second stage is less intense. The transmittance at the minimum is of the order of 50% of the initial value (full line in Fig. 3), corresponding to an effective transient absorption coefficient of 4000 cm⁻¹.

Figure 4 shows the transient intensity transmitted by a

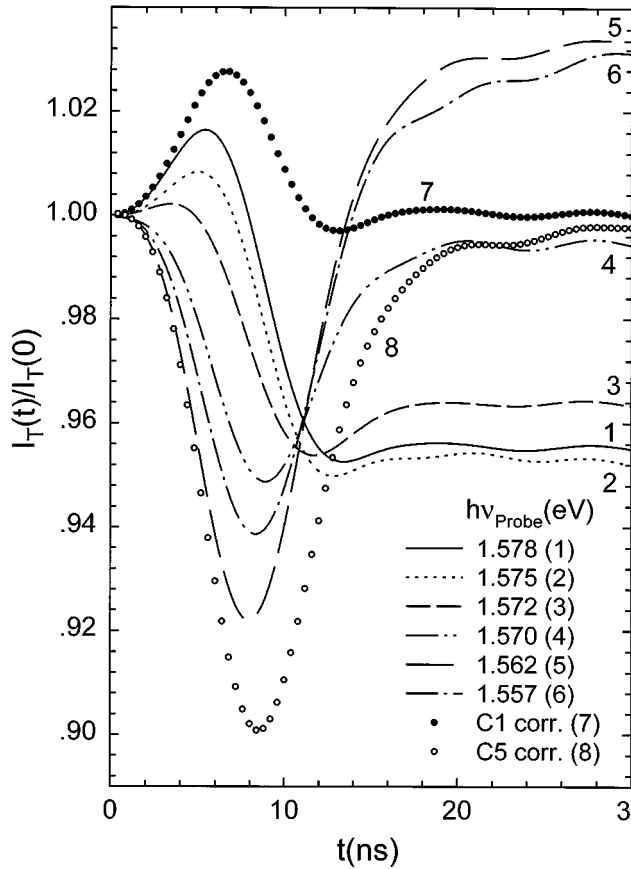


FIG. 4. Transmittancy transients of a 4.42- μm -thick GaSe sample for different probe photon energies, when excited by 532-nm pump pulses with maximum photon flux of 3×10^{24} photons/cm² s. Curves 1–6 (lines) are the experimental transients. Curves 7 and 8 (symbols) correspond to curves 1 and 5, respectively, corrected for thermal effects.

4.42- μm -thick GaSe sample for various photon energies of the probe beam, at pump pulse energies of 0.3 mJ (3×10^{24} photons/cm² s at the pulse maximum). The change in the steady state of the transmittance after the pump pulse has thermal origin and will be discussed at the beginning of Sec. IV. For photon energies above 1.572 eV, a transmittance increase of the order of 2% is observed before the thermal effect dominates. Below this photon energy, a minimum is observed that becomes deeper around 1.565 eV. On the assumption that thermal changes are proportional to the total energy of the pump pulse absorbed by the sample until a given instant, they can be straightforwardly calculated and subtracted from the experimental transient in order to get the electronic contribution. Curves 7 and 8 have been obtained in that way from curves 1 and 5, respectively. From the transmittance at the minima, an effective transient absorption coefficient can be calculated, after correcting for thermal effects. This is shown in Fig. 5(a) (symbols) as a function of the probe photon energy. The full line has been calculated through a model that will be discussed in Sec. IV, in which we will also show that the transmittance increase for photon energies higher than 1.572 eV can be related to the refractive index change associated to the transient absorption [Fig. 5(b)].

Figure 6 shows the effect of the sample temperature on

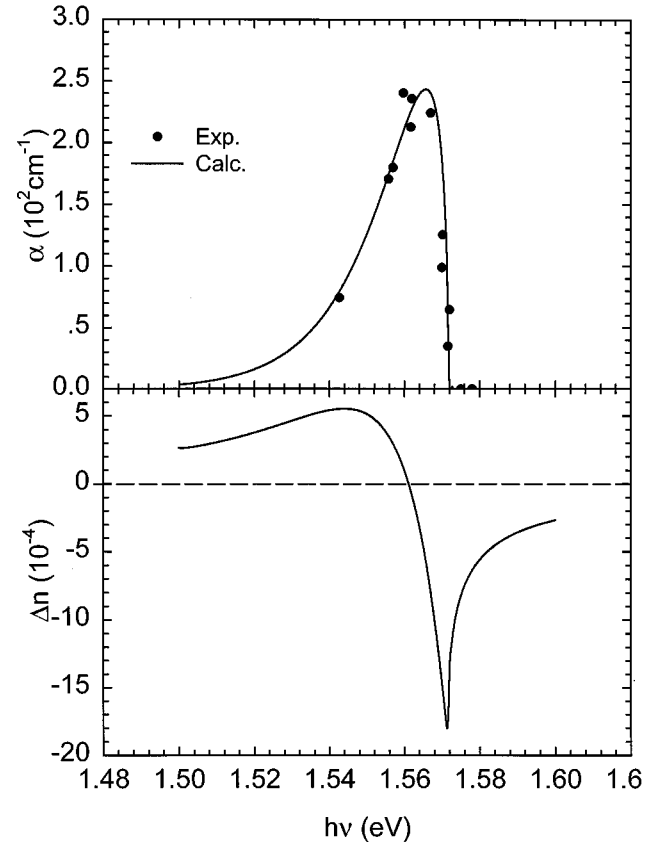


FIG. 5. (a) Transient absorption coefficient at the transmittance minimum as a function of the probe photon energy. Full line: spectral shape calculated through Eq. (9), with $E_0 = 1.5725$ eV, $E_{Fh}^* - E_{0B} = 5k_B T$, and $m_{rBC}^* = 1.05m_0^*$. (b) Spectrum of the refractive index change corresponding to the full line in (a) as calculated through the Kramers-Kronig relation [Eq. (18)].

the transients of Fig. 1. The pump pulse energy was fixed at 5 mJ (5×10^{25} photons/cm² s at the maximum). Heating the sample seems to have the same effect as lowering the pump pulse energy.

In the case of InSe an additional effect can be observed when the pump and probe photon energies are quasidegen-

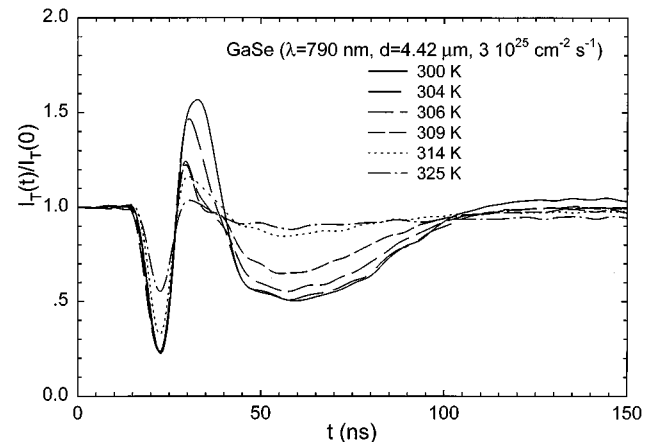


FIG. 6. Transmittancy transients of a 4.42- μm -thick GaSe sample for a 790-nm probe beam, when excited by 532-nm pump pulses with a maximum photon flux of 5×10^{25} photons/cm² s, at different temperatures.

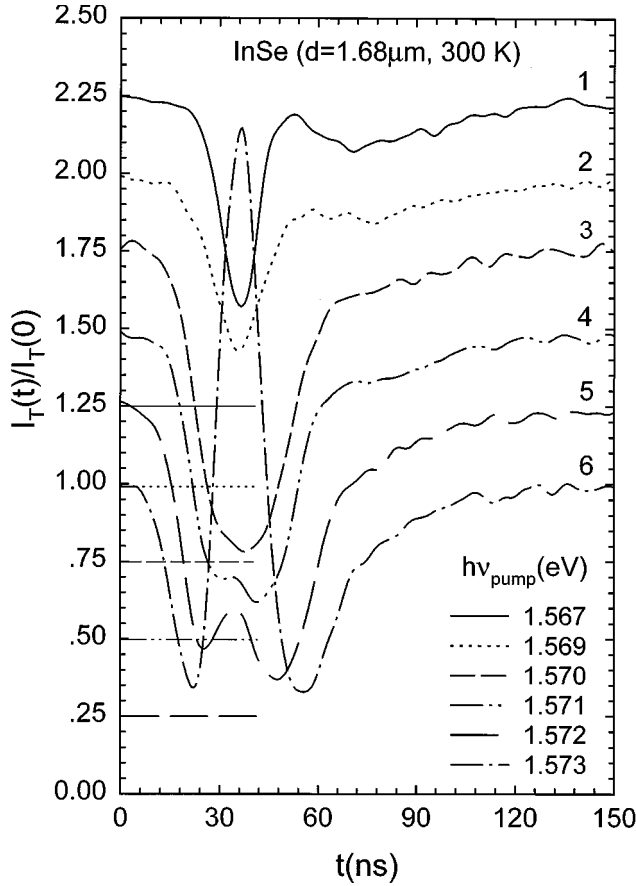


FIG. 7. Transmittancy transients of a 1.68 μm -thick InSe sample for a 790 nm probe beam, when excited by Ti-sapphire pump pulses with a maximum photon flux of 3×10^{25} photons/cm² s and different photon energies. The origin of the ordinate axis has been shifted by 0.25 steps from curve 5 to 1.

erate. Figure 7 shows the transient intensity transmitted by a 1.68- μm -thick InSe sample for several photon energies of the pump pulse generated by a Ti-sapphire laser. For photon energies higher than 1.585 eV or lower than 1.560 eV, the transients are identical to those obtained with 532-nm pulses (Fig. 3). Between these energies, when the photon energy increases from 1.560 eV, the first stage of the transient (intensity decrease) becomes wider and deeper and the second stage disappears. The transmitted intensity at the minimum can be as low as 3% of the initial value (curve 3 in Fig. 7) which corresponds to an effective absorption coefficient of the order of 2×10^4 cm⁻¹. For pump photon energies around 1.573 eV (curve 6 in Fig. 7), a new maximum arises at the center of the transient that can nearly double the transmitted intensity in absence of excitation.

IV. DISCUSSION

Thermal effects due to the sample heating by the pump pulse can obviously affect the time response of the transmitted intensity. As the sample is heated, the refractive index increases and the sample transmittance increases or decreases depending on the probe wavelength. The sample heating is fast and occurs during the pulse, but the cooling can last for several tens of microseconds. Therefore, when thermal effects are observed in the time scale used in these

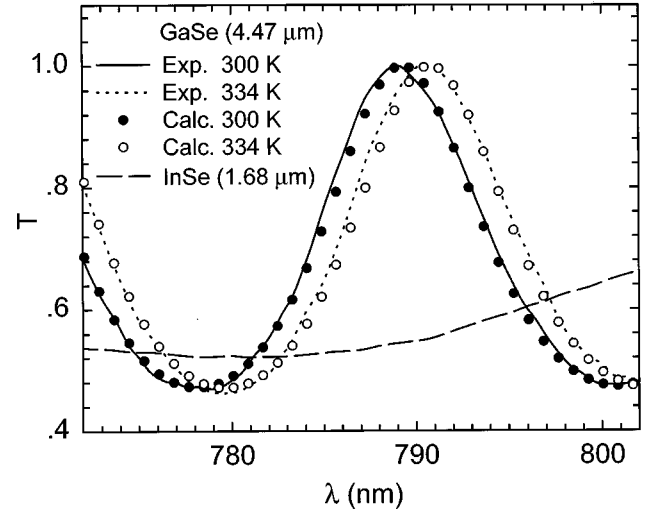


FIG. 8. Transmission spectra of GaSe and InSe samples used in the experiments in the wavelength range of the probe beam. The spectrum of the InSe sample corresponds to 300 K. Spectra of the GaSe sample have been taken at 300 (full line) and 334 K (dotted line). The symbols are the spectra calculated through Eq. (1), with a correction factor of 0.85 for the reflectivity.

experiments, they appear as a change in the final steady state of the transmittance with respect to its value before the pump pulse. In the transparent region, the sample behaves as a Fabry-Pérot interferometer and its transmittance T is given by the well-known Airy function:

$$T = \frac{1}{1 + F \sin^2 \delta}, \quad (1)$$

$$F = \frac{4R}{(1-R)^2}, \quad R = \left(\frac{n-1}{n+1} \right)^2, \quad \delta = \frac{2\pi nd}{\lambda_p},$$

where R is the semiconductor reflectivity for normal incidence, n is the semiconductor refractive index (for light polarization perpendicular to the c axis), λ_p is the probe wavelength, and d is the sample thickness. Figure 8 shows the interference fringe patterns at 300 and 334 K of the 4.42- μm -thick GaSe sample used in transients shown in Figs. 2, 4, and 6. Lines correspond to the experimental spectra. Points have been calculated through Eq. (1) with the refractive index spectra of Ref. 17 and a correction factor of 0.85 for the reflectivity, corresponding to about 3% of scattering losses in each reflection due to surface imperfections. The interference patterns of Fig. 8 give an account of thermal effects observed in the experiments reported here. An interference maximum occurs for $\lambda_{\text{max}} = 789$ nm at 300 K. Curves 1, 2, and 3 in Fig. 4 correspond to a probe wavelength $\lambda_p < \lambda_{\text{max}}$ and the thermal transient is negative. Curve 4 corresponds to a wavelength very close to λ_{max} and the thermal change is very small. For curves 5 and 6, $\lambda_p > \lambda_{\text{max}}$ and the thermal change is positive. The thermal increase of the refractive index can be estimated from the transmittance change and turns out to be $\Delta n \approx 0.0022$, corresponding to a temperature increase of 12 °C.¹⁷ For time responses shown in Figs. 2 and 6 the probe wavelength is also very close to λ_{max} and thermal effects are very weak.

The transmission spectrum of the InSe sample is also shown in Fig. 8. It is apparent that, in the wavelength interval close to the probe, the slope $dT/d\lambda$ is much smaller than for the GaSe sample. This is due to the fact that the sample is thinner and the light is partly absorbed. Consequently, thermal or electronic changes of the refractive index can hardly affect the sample transmittance.

Let us now discuss the effect of the probe wavelength on the transient absorption. The key to the physical interpretation of the results reported in Sec. III is the band structure of layered III-VI selenides. The inset of Fig. 1 shows a sketch of the band structure of GaSe in the center of the Brillouin zone. The valence bands are named *A*, *B*, and *C*, according to the notation of Kuroda, Munakata, and Nishina.²¹ The uppermost one (*B*) has mainly a Se p_z character, with a small component being Se p_x - p_y , which makes the fundamental transition to the *s*-character conduction band weakly allowed for light polarization perpendicular to the *c* axis. The bands *A* and *C*, mainly with Se p_x - p_y character, are deeper than *B* due to the crystal-field anisotropy (the Coulomb attraction of Se p_x - p_y electrons with In cations is much larger than that of Se p_z electrons).^{21,22} On the other hand, bands *A* and *C* are split because of the spin-orbit interaction. The corresponding band scheme of InSe is nearly identical to that of Fig. 1, besides the value of the band gap (1.27 eV for InSe at RT). The transition from *A* or *C* to *B* is allowed by crystal symmetry for light polarization perpendicular to the *c* axis, but cannot be observed in the linear optical regime because there are no empty states in band *B*. Things are different when an intense pump pulse is present. In experiments reported in Sec. III, the photon energy of the pump pulse is higher than the band gap, but electrons (holes) are thermalized to the minimum (maximum) of the conduction (valence) band in a time much shorter than the duration of the pump pulse. Then, the top of band *B* is emptied and the transition from *C* to *B* can be observed. The energy difference $E_{vB} - E_{vC}$ is about 1.56 eV in both semiconductors, close to the probe photon energy. Then, results of Sec. III can be interpreted as an absorption of the probe light by electrons of band *C* that are excited to the empty states of band *B*, created by the pump pulse.

We could also attempt to interpret our results through a model involving transitions of nonequilibrium electrons in the conduction band to upper conduction bands. This would not affect the formalism developed in the rest of this section. Nevertheless, the model involving inter-conduction-band transitions would imply hypothesis concerning the conduction-band structure of InSe and GaSe, as the effects reported here occur in both semiconductors at the same photon energy. All spectroscopic data and band-structure calculations confirm the similarity between the uppermost valence bands of both compounds. On the other hand, the spectroscopic data reveal differences between InSe and GaSe in the arrangement and energies of the conduction-band states.

Let us determine the spectral shape of the transient absorption. Figure 9 shows a density-of-states scheme in which the degenerate electron (hole) gas created by the pump pulse is represented by the quasi-Fermi level and the occupied (empty) states in the conduction (valence) band. We will

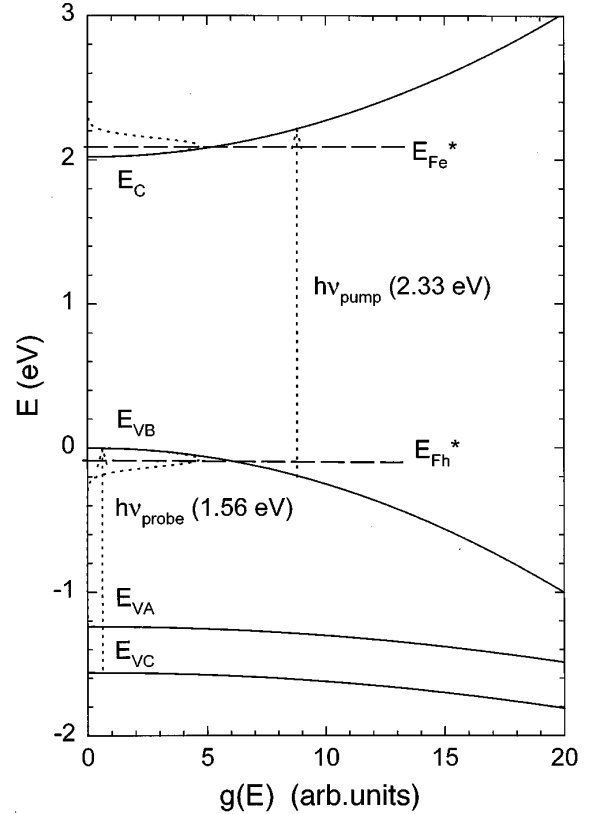


FIG. 9. GaSe density-of-states band scheme: the degenerate electron (hole) gas created by the pump pulse is represented by the quasi-Fermi level and the occupied (empty) states in the conduction (valence) band.

assume, for simplicity, isotropic bands with parabolic dispersion relation $E(k)$. Near to the maxima the $E(k)$ relations are

$$E_{vB}(k) = E_{0vB} - \frac{\hbar^2 k^2}{2m_{vB}^*}, \quad (2)$$

$$E_{vC}(k) = E_{0vC} - \frac{\hbar^2 k^2}{2m_{vC}^*}.$$

Let us assume that $m_{vC}^* > m_{vB}^*$, which is coherent with recent linear muffin-tin orbital band-structure calculations.²⁵ In an optic direct transition the energy conservation implies

$$E_{vB}(k) = E_{vC}(k) + \hbar\omega. \quad (3)$$

If we define $E_0 = E_{0vB} - E_{0vC}$ and a reduced mass m_{rBC}^* :

$$\frac{1}{m_{rBC}^*} = \frac{1}{m_{vB}^*} - \frac{1}{m_{vC}^*}, \quad (4)$$

then, the energy conservation condition can be written

$$E_0 - \hbar\omega = \frac{\hbar^2 k^2}{2m_{rBC}^*}. \quad (5)$$

It must be outlined that the reduced mass is higher than m_{vB}^* . In fact it will be infinite if $m_{vB}^* = m_{vC}^*$, reflecting the fact that, in this case, the transition between bands *C* and *B* would occur only at a photon energy $\hbar\omega = E_0$.

The absorption coefficient for a direct transition between C and B is given by the following expression:²⁶

$$\alpha_{CB} = \frac{\pi e^2}{\epsilon_0 c n m_0^2 \omega} |P_{CB}|^2 \int d\tau_k \frac{1}{4\pi^3} \times \delta \left[\hbar\omega - E_0 + \frac{\hbar^2 k^2}{2m_{rBC}^*} \right] F_{VC} (1 - F_{VB}). \quad (6)$$

P_{CB} is the dipole matrix element between bands C and B , F_{VC} is the occupation probability of states in band C , which can be assumed to be 1, and $1 - F_{VB}$ is the probability of the final state in band B to be empty, which can be written as a function of the hole quasi-Fermi level:

$$1 - F_{VB} = \frac{1}{1 + e^{(E_{Fh}^* - E_{0VB}(k))/k_B T}}. \quad (7)$$

Using Eq. (5), we can write

$$E_{Fh}^* - E_{VB}(k) = E_{Fh}^* - E_{0VB} + \frac{\hbar^2 k^2}{2m_{VB}^*} = E_{Fh}^* - E_{0VB} + \frac{m_{rBC}^*}{m_{VB}^*} (E_0 - \hbar\omega). \quad (8)$$

Let us define the oscillator strength of the CB transition $f_{CB} = 2|P_{CB}|^2 / (m_0 \hbar \omega)$. After integration in the k space and rearrangement of constants, Eq. (6) yields the absorption coefficient

$$\alpha_{CB}(\hbar\omega) = \frac{4\omega}{cn} \left(\frac{m_{rBC}^*}{m_0} \right)^{3/2} f_{CB} \frac{R_0^{1/2}}{\hbar\omega} \times \frac{E_0 - \hbar\omega}{1 + e^{(E_{Fh}^* - E_{0B})/k_B T} e^{(m_{rBC}^*/m_{VB}^*)(E_0 - \hbar\omega)/k_B T}}, \quad (9)$$

where R_0 is the Rydberg constant. The fact that the absorption edge appears at energies below a certain E_0 is a consequence of the assumption $m_{VC}^* > m_{VB}^*$.

The oscillator strength f_{CB} of this transient absorption can be estimated from the f -sum rule,²⁷

$$\int_0^\infty \omega \varepsilon''(\omega) d\omega = \frac{\pi}{2} \omega_p^2, \quad (10)$$

which establishes the constancy of the total oscillator strength in the electron gas. Let us consider the band structure shown in Figs. 1 and 9. The shape of the absorption edge from the C valence band to the conduction band would be affected by the filling of the conduction band due to the pump pulse. Taking into account the band-filling effects (but not considering the electron-hole interaction) this absorption edge would be given by an expression similar to Eq. (9):

$$\alpha_{CC}(\hbar\omega) = \frac{4\omega}{cn} \left(\frac{m_{rCC}^*}{m_0} \right)^{3/2} f_{CC} \frac{R_0^{1/2}}{\hbar\omega} \times \frac{\hbar\omega - E_1}{1 + e^{(E_{Fe}^* - E_{0c})/k_B T} e^{-(m_{rCC}^*/m_c^*)(\hbar\omega - E_1)/k_B T}} = \frac{\alpha_{CC}^0(\hbar\omega)}{1 + e^{(E_{Fe}^* - E_{0c})/k_B T} e^{-(m_{rCC}^*/m_c^*)(\hbar\omega - E_1)/k_B T}}, \quad (11)$$

where we have introduced the reduced effective mass $m_{rCC}^* = 1/m_{VC}^* + 1/m_c^*$, oscillator strength f_{CC} , and energy gap $E_1 = E_{0C} - E_{0VC}$ between the valence band C and the conduction band, and the quasi-Fermi level of electrons in the conduction band E_{Fe}^* . In absence of excitation, this expression reduces to the well-known absorption edge for direct allowed transitions. In the presence of strong excitation, the absorption coefficient decreases, especially for photon energies between E_1 and E_{Fe}^* . The absolute decrease of the absorption coefficient $\Delta\alpha_{CC}(\hbar\omega) = \alpha_{CC}^0(\hbar\omega) - \alpha_{CC}(\hbar\omega)$ will be given by

$$\Delta\alpha_{CC}(\hbar\omega) = \frac{\alpha_{CC}^0(\hbar\omega)}{1 + e^{(E_{0c} - E_{Fe}^*)/k_B T} e^{(m_{rCC}^*/m_c^*)(\hbar\omega - E_1)/k_B T}}. \quad (12)$$

If we express the f -sum rule in a function of the absorption coefficient $\alpha(\omega) = \omega \varepsilon''(\omega) / cn$, and neglect the refractive-index change in the interval through which α_{CB} and $\Delta\alpha_{CC}$ are different than zero, we can write

$$\frac{1}{n_{E_0}} \int_{-\infty}^{E_0} \alpha_{CB}(\hbar\omega) d(\hbar\omega) = \frac{1}{n_{E_1}} \int_{E_1}^{\infty} \Delta\alpha_{CC}(\hbar\omega) d(\hbar\omega). \quad (13)$$

Let us introduce the following variables and parameters:

$$u = \frac{m_{rCB}^*}{m_{VB}^*} \frac{E_0 - \hbar\omega}{k_B T}, \quad v = \frac{m_{rCC}^*}{m_c^*} \frac{\hbar\omega - E_1}{k_B T},$$

$$a = \frac{E_{Fh}^* - E_{0VB}}{k_B T}, \quad b = \frac{E_{0C} - E_{Fe}^*}{k_B T}.$$

Using these variables in the expressions of the absorption coefficients, Eq. (13) becomes

$$\frac{f_{CB}}{n_{E_0}^2} \int_0^\infty \frac{u^{1/2} du}{1 + e^{u-a}} = \frac{f_{CC}}{n_{E_1}^2} \int_0^\infty \frac{v^{1/2} dv}{1 + e^{v-b}}. \quad (14)$$

From the definition of parameters a and b , it follows that

$$\frac{\Delta p}{N_V} \frac{1}{n_{E_0}^2} f_{CB} = \frac{\Delta n}{N_C} \frac{1}{n_{E_1}^2} f_{CC}, \quad (15)$$

where $\Delta n = \Delta p$ are the densities of photoexcited carriers. Finally, f_{CB} is given by

$$f_{CB} = \left(\frac{n_{E_0}}{n_{E_1}} \right)^2 \left(\frac{N_V}{N_C} \right) f_{CC} = \left(\frac{n_{E_0}}{n_{E_1}} \right)^2 \left(\frac{m_{VB}^*}{m_c^*} \right)^{3/2} f_{CC}. \quad (16)$$

TABLE I. Values of the semiconductor parameters involved in Eq. (16) for GaSe and InSe.

| | E_g (eV) | $\frac{m_c^*}{m_0}$ | $\frac{m_v^*}{m_0}$ | E_1 (eV) | n_{E1} | f_{CC} | E_0 (eV) | n_{E0} | f_{CB} |
|------|-------------------|---------------------|---------------------|---------------------------|------------------|-------------------|---------------------------|---------------------------|----------|
| InSe | 1.25 (Ref. 19) | 0.12 (Ref. 31) | 0.45 (Ref. 32) | 2.75 (Refs. 19 and 21) | 3.6 (Ref. 19) | 2.85 (Ref. 21) | 1.55 (Refs. 19 and 21) | 2.85 (Refs. 19 and 20) | 12.8 |
| GaSe | 2.00 (Ref. 17) | 0.18 (Ref. 17) | 0.50 (Ref. 17) | 3.55 (Ref. 16) | 4 (Ref. 16) | 2.80 (Ref. 16) | 1.55 (Refs. 16 and 17) | 2.90 (Ref. 17) | 6.2 |

Equation (16) indicates that, in fact, the appearance of the transient inter-valence-band absorption can be considered as a direct consequence of the f -sum rule. As the absorption coefficient of the transition from valence band C to the conduction band decreases due to the conduction-band filling, the subsequent loss of oscillator strength is compensated by the appearance of a new transition from valence band C to the empty states of valence band B . According to studies of optical nonlinearities in the fundamental absorption edge of GaSe,^{11–13} exciton screening and band-filling effects are observed at excitation rates ranging from 10^{24} to 2×10^{25} photons/cm² s, that are of the same order as those used in the experiments reported in Sec. III. In GaAs,²⁸ exciton screening and band filling effects are observed at lower excitation rates (from 10^{22} to 10^{24} photons/cm² s) owing to the larger exciton radius and lower conduction-band effective mass with respect to GaSe.

Table I gives the values of f_{CC} found in literature, as well as the other parameters involved in Eq. (16), and the estimation of f_{CB} for GaSe and InSe. With this estimation of the oscillator strength, Eq. (9) can give quantitative account of inter-valence-band transitions. In absence of excitation, $E_{Fh}^* - E_{0B}$ is positive and very large and no absorption is observed. In the presence of a pump pulse yielding a degenerate hole gas in valence band B , $E_{Fh}^* - E_{0B}$ is negative and absorption appears in the spectral range through which the sum of exponents in the denominator of Eq. (9) is negative. If the upper limit is E_0 , the lower limit would be of the order of

$$\hbar \omega_{\min} = E_0 - \frac{m_{VB}^*}{m_{rBC}^*} (E_{0VB} - E_{Fh}^*). \quad (17)$$

If the hole gas in valence band B is not completely degenerate, the absorption coefficient is proportional to the hole concentration and the FWHM of the absorption peak is of the order of $(m_0/m_{rBC}^*)k_B T$.

Now we are in condition to fit the expression of the transient absorption given by Eq. (9) to the experimental results of Fig. 5(a). The full line in Fig. 5(a) has been calculated through Eq. (9), with $E_0 = 1.572$ eV, $m_{rBC}^* = 1.05m_0^*$, and $E_{Fh}^* - E_{0B} = 5k_B T$, corresponding to a hole concentration of the order of 10^{17} cm⁻³. This is coherent with the fact that the FWHM of the absorption peak is of the order of $k_B T$, indicating that the hole gas in valence band B is not completely degenerate (the full degeneracy in GaSe valence band is not attained until hole concentrations higher than 10^{20} cm⁻³). Nevertheless, with the excitation rates used in transients of Fig. 4 and the carrier lifetimes found in the literature,²⁹ the

hole concentration should be of the order of 5×10^{18} to 10^{19} cm⁻³. The origin of this disagreement can be due to the following factors.

(i) On the one hand, we have calculated the effective absorption coefficient on the assumption of a homogeneous excitation of the sample, which is not the case. The fact that in a much thinner InSe sample the effective absorption coefficient is higher suggests that the transient absorption occurs in a thin layer near the sample surface.

(ii) On the other hand, we have assumed the occupation probability of band C to be 1, which is not necessarily true when the probe beam is a laser and the nonlinear absorption coefficient is very high. In fact, as we will see at the end of this section, in these conditions, stimulated emission from band B to C can affect the probe intensity transmitted by the sample. Unfortunately, the gain limitations of the broadband detector used in our experiments prevented us from studying the transient absorption at lower probe intensities.

With these reserves, the fact that the spectral response of the effect reported here follows Eq. (9) confirms our assumption. The decrease of the probe intensity in the first stage of the time responses shown in Figs. 2–7 would be due to the appearance of a transient allowed transition between bands C and B as the top of band B is emptied by the pump pulse.

The appearance of a transient absorption peak necessarily leads to a transient change in the refractive index. Figure 5(b) shows the refractive index change corresponding to an absorption peak with the intensity and spectral shape of the continuous line of Fig. 5(a) as calculated through the Kramers-Kronig relation:²⁶

$$\Delta n(E) = \frac{\hbar c}{\pi} P \int_{-\infty}^{E_0} \frac{\alpha_{CB}(E')}{E'^2 - E^2} dE'. \quad (18)$$

For photon energies slightly higher than 1.572 eV, the refractive index change is $\Delta n \approx -0.0015$. This can give an account of the transmittancy increase observed in curves 1 and 2 of Fig. 4 at the beginning of the pulse. In this curve a thermal increase of the index $\Delta n \approx -0.0022$ results in a transmittancy decrease of 4.6%. Coherently, an electronic decrease of the index $\Delta n \approx -0.0015$ results in a transmittancy increase close to 3% at the maximum [curve 7 in Fig. 5(a)].

Results of Fig. 6 can also be understood through Eq. (9). As temperature increases, E_0 decreases¹⁹ and the photon energy becomes closer to the upper absorption edge [Fig. 5(a)], which results in a lower absorption of the probe.

Coulomb attraction in the degenerate electron-hole gas created by the pump pulse allows for an explanation of the

onset of the second stage of the transients, as it leads to a reduction of the band gap. This allows the *B* band to move up in energy, as the electron and hole concentrations increase, which “detunes” the photon energy of the probe with respect to E_0 . In Eq. (9), as E_0 increases, the absorption coefficient decreases, which corresponds to the fact that, as band *B* moves up, the final state that fulfills the energy conservation is deeper in the band and then, its occupation probability is higher. Nevertheless, the decrease of α_{CB} explains the onset of the second stage but not the subsequent increase of the transmitted intensity well above the initial value. A transient change in the refractive index due to the transient

absorption cannot account for that increase because in all transients shown in Figs. 2 and 6, the probe wavelength corresponds to an interference maximum and any refractive index change would result in a transmittance decrease.

An alternative explanation can be found in the possibility of an amplification of the probe beam by stimulated emission in the sample. If stimulated emission is included, the effective absorption coefficient is also calculated from Eq. (5) but the occupation number factor is now $F = F_C(1 - F_B) - F_B(1 - F_C) = F_C - F_B$. Then, with the energy conservation condition [Eq. (3)], the absorption coefficient can be written as

$$\alpha_{CB}(\hbar\omega) = \frac{4\omega}{cn} \left(\frac{m_{rBC}^*}{m_0} \right)^{3/2} f_{CB} \frac{R_0^{1/2}}{\hbar\omega} \sqrt{E_0 - \hbar\omega} \left[\frac{1}{1 + e^{(E_{0C} - E_{FC}^*)/k_B T}} e^{-(m_{rBC}^*/m_{VB}^*)(E_0 - \hbar\omega)/k_B T} - \frac{1}{1 + e^{(E_{0B} - E_{Fh}^*)/k_B T}} e^{-(m_{rBC}^*/m_{VB}^*)(E_0 - \hbar\omega)/k_B T} \right], \quad (19)$$

where we have introduced the quasi-Fermi level of holes in valence band *C*, E_{FC}^* . The sign of the effective absorption coefficient depends of the sign of the last parenthesis. It is easy to show that it is negative if $E_{Fh}^* - E_{FC}^* > \hbar\omega$, which means that, in that case, the stimulated emission dominates. If we assume that band *B* moves up due to Coulomb attraction, the quasi-Fermi level E_{Fh}^* follows the band and the condition for amplification of the probe beam is fulfilled at a certain level of excitation. The second stage of the transient of Fig. 2 would then correspond to the amplification of the probe beam by stimulated emission.

Results of Fig. 7 confirm this interpretation. When the photon energy of the pump is close to E_0 , a part of the pump flux can also contribute to the transitions from *C* to *B*. As a result, a high concentration of holes is created in band *C* and the hole concentration in band *B* decreases, i.e., holes are redistributed among bands *C* and *B*. In this case, the Coulomb attraction would act between electrons in the conduction band and holes in both bands and the detuning effect would be less effective. This is the situation in which the decrease of intensity in the first stage becomes larger and more intense (curve 3 in Fig. 5). On the other hand, at energies very close to resonance, the hole concentration in band *C* becomes very large. Then the stimulated emission condition is fulfilled and the probe beam is amplified (curve 6 in Fig. 7).

The nonlinear absorption and the measured transmittance transients can be accounted for from carrier kinetics differential equations, with a few simplifying assumptions. The recombination of holes in the uppermost valence band is assumed to be controlled by a nonlinear equation:

$$\frac{dp_B}{dt} = \Phi_{\text{Pump}}(t) \alpha_0 - \kappa p^2 - \frac{dp_C}{dt}, \quad (20)$$

where $\Phi_{\text{Pump}}(t)$ is the pump photon flux, α_0 the absorption coefficient of the material for the pump photon energy, and κ the electron-hole quadratic recombination coefficient. The last term must be included as holes in band *C* are created by electron transitions to the empty states of band *B*. On the other hand, the recombination of holes in the *C* valence band is assumed to be linear,

$$\frac{dp_C}{dt} = \Phi_{\text{Probe}} \alpha_{\text{NL}}(p_B, p_C, \hbar\omega) - \frac{p_C}{\tau_C}, \quad (21)$$

where Φ_{Probe} is the probe photon flux, α_{NL} the valence-band to valence-band nonlinear absorption coefficient given by Eq. (19), and τ_C the lifetime of holes in band *C*. This differential equation is nonlinear as the absorption coefficient depends on the hole concentrations p_B and p_C . Both differential equations can be numerically solved. The band-gap renormalization due to Coulomb attraction, which gives rise to the increase of E_0 in Eq. (19), has been included in the calculation through the parametric expression given by Vashishta and Kalia.³⁰ Figure 10 shows the results of a calculation in which the pump pulse shape and energy (including secondary pulses), as well as the probe intensity, have been assumed to be those corresponding to the experimental conditions. The effective mass in band *C* has been taken so as to give the reduced mass $m_{rBC}^* = 1.05m_0$, which is the value estimated from the spectral shape of the transient absorption [Fig. 5(a)]. The electron-hole quadratic recombination coefficient κ and the lifetime of holes in band *C* τ_C have been taken as free parameters.

The main features of the experimental results are reproduced in the calculated response shown in Fig. 10, with the parameter values given in the legend. It must be outlined that the shape of the calculated response is very sensitive to the lifetime of holes in band *C*. A shorter lifetime (5 ns) makes

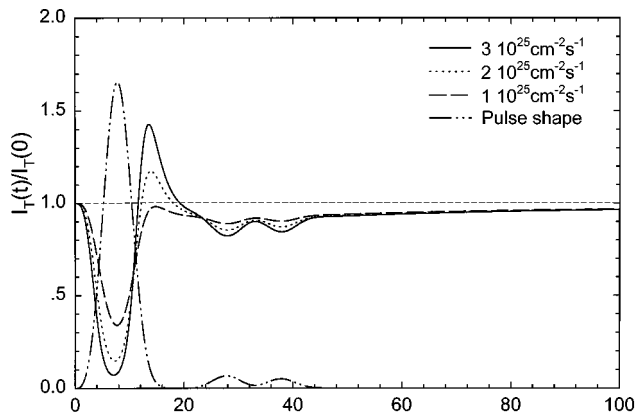


FIG. 10. Transmittance transients calculated through Eqs. (19)–(21), with the following values for parameters: $m_B^* = 0.5m_0$, $m_C^* = 0.95m_0$, $\kappa = 2.5 \times 10^{-11} \text{ cm}^3/\text{s}$, $\tau_C = 10 \text{ ns}$.

the second stage of the response (corresponding to the probe amplification) disappear. A longer lifetime (15 ns) makes this stage become much more intense than that experimentally observed. On the other hand, quadratic electron-hole recombination must be assumed in order to give an account of the third stage of the experimental transient of Fig. 2 (slowly decreasing absorption of the probe). This third stage is reproduced even if secondary pulses of the pump are not included. On the other hand, if electron-hole recombination is assumed to be linear this stage cannot be reproduced.

V. CONCLUSIONS

Strong nonlinear optical effects at photon energies corresponding to the transition from a lower-energy valence band to the uppermost one have been shown to occur in GaSe and InSe when the edge of the latter band is emptied by an optical pulse. The intensity and spectral shape of the transient absorption has been quantitatively accounted for and shown to depend on the hole quasi-Fermi level and reduced effective mass between both bands. An estimation of the oscillator strength of the inter-valence-band transition has been made through the f -sum rule. The transmission transients could also be interpreted through carrier kinetics equations including stimulated emission and renormalization of the band gap due to Coulomb interaction in the electron-hole degenerate gas.

These results open the way to a better understanding of the valence-band structure in III-VI layered compounds and can certainly be extended to other semiconductor compounds. Time-resolved spectroscopy of these effects in the femtosecond range can also yield valuable information about hole thermalization processes in III-VI compounds.

ACKNOWLEDGMENTS

This work was supported by the Spanish Government under Grant No. MAT95-0391 and by Generalitat Valenciana under Grant Nos. GV-2505/94 and 3235/95.

*Present address: ESPCI, Laboratoire de Physique du Solide, 10 Rue Vauquelin, 75231 Paris, Cedex 05, France.

¹G. A. Akhundov, A. A. Agaeva, V. M. Salmanov, Yu. P. Sharonov, and I. D. Yaroshetskii, *Fiz. Tek. Poluprovodn.* **7**, 1229 (1972) [*Sov. Phys. Semicond.* **7**, 826 (1973)].

²V. I. Sokolov, Yu. F. Solomonov, and V. K. Sobashiev, *Fiz. Tverd. Tela Leningrad* **17**, 1914 (1975) [*Sov. Phys. Solid State* **17**, 1256 (1976)].

³I. M. Catalano, A. Cingolani, A. Minafra, and C. Paorici, *Opt. Commun.* **24**, 105 (1978).

⁴Yu. F. Solomonov and V. K. Sobashiev, *Phys. Status Solidi A* **74**, 75 (1982).

⁵G. B. Abdullaev, K. R. Allakhverdiev, M. E. Karaseev, V. I. Konov, L. A. Kulevskii, N. B. Mustafaev, P. P. Pashinin, A. M. Prokhorov, Yu. M. Starodunov, and N. I. Chapliev, *Kvant. Electron* **16**, 725 (1989) [*Sov. J. Quantum Electron.* **19**, 494 (1989)].

⁶E. Bringuier, A. Bourdon, N. Piccioli and A. Chevy, *Phys. Rev. B* **49**, 16 971 (1994).

⁷K. L. Vodopyanov, L. A. Kulevskii, V. G. Voevodin, A. I. Gribenyukov, K. R. Allakhverdiev, and T. A. Kerimov, *Opt. Commun.* **83**, 322 (1991).

⁸A. Bianchi, A. Ferrario, and M. Musci, *Opt. Commun.* **25**, 256 (1978).

⁹J. L. Oudar, Ph. J. Kupecek, and D. S. Chemla, *Opt. Commun.* **29**, 119 (1979).

¹⁰Ph. J. Kupecek, H. Le Person, and M. Comte, *Infrared Phys.* **19**, 263 (1979).

¹¹G. P. Golubev, V. S. Dneprovskii, Z. D. Kovalyuk, and V. A. Stadnik, *Fiz. Tverd. Tela Leningrad* **27**, 432 (1985) [*Sov. Phys. Solid State* **27**, 265 (1985)].

¹²A. M. Bakiev, Yu. V. Vandishev, G. S. Volkov, V. S. Dneprovskii, Z. D. Kovalyuk, A. R. Lesiv, S. V. Savinov, and A. I. Furtichev, *Fiz. Tverd. Tela Leningrad* **28**, 1035 (1986) [*Sov. Phys. Solid State* **28**, 579 (1986)].

¹³V. S. Dneprovskii, A. I. Furtichev, V. I. Klimov, E. V. Nazvanova, D. K. Okorokov, and V. U. Vandishev, *Phys. Status Solidi A* **146**, 341 (1988).

¹⁴C. Hirllmann, J. F. Morhange, M. A. Kanehisa, A. Chevy, and C. H. Brito Cruz, *Appl. Phys. Lett.* **55**, 2307 (1989).

¹⁵I. M. Catalano, A. Cingolani, C. Cali, and S. Riva-Sanseverino, *Solid State Commun.* **30**, 585 (1979).

¹⁶Y. Sasaki, C. Hamaguchi, and J. Nakai, *J. Phys. Soc. Jpn.* **38**, 162 (1975); **38**, 169 (1975).

¹⁷R. Le Toullec, M. Piccioli, M. Mejatty, and M. Balkanski, *Nuovo Cimento B* **38**, 159 (1977).

¹⁸J. Camassel, P. Merle, H. Mathieu, and A. Chevy, *Phys. Rev. B* **17**, 4718 (1978).

¹⁹M. Piacentini, E. Doni, R. Girlanda, V. Grasso, and A. Balzarotti, *Nuovo Cimento B* **54**, 269 (1979).

²⁰R. Le Toullec, N. Piccioli, and J. C. Chervin, *Phys. Rev. B* **22**, 6162 (1980).

²¹N. Kuroda, I. Munakata, and Y. Nishina, *Solid State Commun.* **33**, 687 (1980).

²²N. Kuroda and Y. Nishina, *Physica B & C* **105**, 30 (1981).

²³N. Piccioli, R. Le Toullec, F. Bertrand, and J. C. Chervin, *J. Phys. (Paris)* **42**, 1129 (1981).

²⁴N. Kuroda, O. Ueno, and Y. Nishina, *J. Phys. Soc. Jpn.* **55**, 581 (1986).

²⁵C. Ulrich, A. R. Goñi, K. Syassen, O. Jopsen, A. Cantarero, and

- V. Muñoz, *Proceedings of the Joint XV AIRPAT and XXXIII EHPGR International Conference, Warsaw, 1995* (World Scientific, Singapore, 1996), p. 612.
- ²⁶O. Madelung, *Introduction to Solid State Theory* (Springer-Verlag, Berlin, 1981).
- ²⁷M. Altarelli, D. L. Dexter, H. M. Nussenzveig, and D. Y. Smith, *Phys. Rev. B* **6**, 4502 (1972).
- ²⁸Y. H. Lee, A. Chavez-Pirson, S. W. Koch, H. M. Gibbs, S. H. Park, J. Morhange, A. Jeffery, N. Peyghambarian, L. Banyai, A. C. Gossard, and W. Wiegmann, *Phys. Rev. Lett.* **57**, 2446 (1986).
- ²⁹V. Augelli, C. Manfredotti, R. Murri, R. Piccolo, and L. Vasanelli, *Phys. Rev. Lett.* **18**, 5484 (1978).
- ³⁰P. Vashishta and K. Kalia, *Phys. Rev. B* **25**, 6492 (1982).
- ³¹E. Kres-Rogers, R. J. Nicholas, J. C. Portal, and A. Chevy, *Solid State Commun.* **44**, 379 (1982).
- ³²Ch. Ferrer-Roca, A. Segura, M. V. Andrés, J. Pellicer, and V. Muñoz, *Phys. Rev. B* **55**, 6981 (1997).